# Realizing a Kondo-Correlated State with Ultracold Atoms

Johannes Bauer,[1] Christophe Salomon,[2] and Eugene Demler[1]

[1]*Department of Physics, Harvard University, Cambridge, Massachusetts 02138, USA*

[2]*Laboratoire Kastler Brossel, CNRS, UPMC, Ecole Normale Superieure, 24 rue Lhomond, 75231 Paris, France*

(Received 15 August 2013; revised manuscript received 30 September 2013; published 20 November 2013)

We propose a novel realization of Kondo physics with ultracold atomic gases. It is based on a Fermi sea of two different hyperfine states of one atom species forming bound states with a different species, which is spatially confined in a trapping potential. We show that different situations displaying Kondo physics can be realized when Feshbach resonances between the species are tuned by a magnetic field and the trapping frequency is varied. We illustrate that a mixture of $^{40}$K and $^{23}$Na atoms can be used to generate a Kondo-correlated state and that momentum resolved radio frequency spectroscopy can provide unambiguous signatures of the formation of Kondo resonances at the Fermi energy. We discuss how tools of atomic physics can be used to investigate open questions for Kondo physics, such as the extension of the Kondo screening cloud.

DOI: 10.1103/PhysRevLett.111.215304 PACS numbers: 67.85.Pq, 72.10.Fk, 72.15.Qm, 75.20.Hr

*Introduction.*—Significant advances in quantum optics, such as in cooling, trapping, and manipulating ultracold atoms, have lead to the realization of a plethora of exciting many-body phases in a controlled manner [1,2]. An important drive for this field is that many of these phases and their description in terms of model Hamiltonians are of great interest in condensed matter physics, such that a fruitful interplay of these fields has developed. It has, for instance, been possible to realize superfluid phases both in fermionic and bosonic systems and the transition to a Mott insulating regime [3–8].

An intriguing many-body effect in condensed matter physics is the Kondo effect. It occurs when itinerant fermions interact with magnetic impurities, such as, for instance, a small concentration of Fe in Au. The orbital occupation of the impurity must be such that there is an unscreened spin present, i.e., in the simplest case a localized state occupied by a single electron. The essence of the Kondo effect is then that at low temperature this electron spin forms a many-body bound state with the itinerant electrons and becomes magnetically screened. Crucial for this magnetic screening are second-order processes which lead to frequent spin flips. This Kondo-correlated state leads to a distinctive feature in the resistivity (Kondo minimum) and was also observed as enhanced transport in quantum dots [9,10].

In spite of decades of intense research [11], there remain unresolved questions. For instance, a Kondo screening cloud with a certain spatial extent and characteristic oscillations was predicted [11–14]; however, its experimental observation has remained elusive. On increasing the impurity concentration from very few to a full lattice, the Kondo clouds overlap and the localized spins interact with each other via the so-called Ruderman-Kittel-Kasuya-Yoshida (RKKY) coupling, mediated by the itinerant fermions. This generates a competing effect to the Kondo screening and leads to a transition to a magnetically ordered state of the spins. The Kondo lattice problem is of paramount importance for the understanding of heavy fermion systems and quantum criticality [15,16]; however, it is very hard to analyze it theoretically beyond the mean field level. Here, we propose an experimental setup based on ultracold atoms to realize single impurity and lattice Kondo situations. The Kondo scale is shown to be accessible by current experimental techniques.

In the field of ultracold atoms, a lot of progress has recently been made for manipulating mixtures of different species that offer the unique possibility to selectively trap one species and to handle heteronuclear Feshbach resonances producing molecular bound states [17–22]. These developments are important ingredients for our proposal. The main idea is to allow atoms of a Fermi sea to form bound states with a different, spatially confined atom, the impurity [see Fig. 1(a)]. We consider two species of

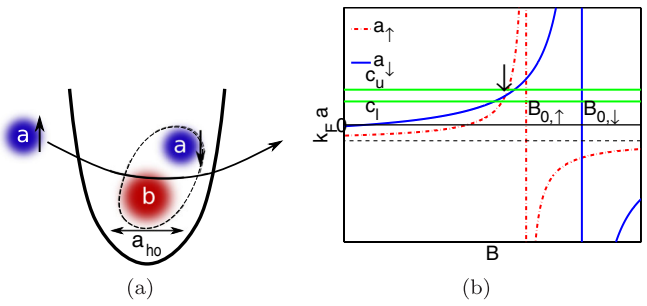


FIG. 1 (color online). (a) Schematic picture of an atomic bound state of an $a$ species atom with a $b$ species atom in a harmonic trap with oscillator length $a_{\mathrm{ho}}$. (b) Schematic plot of the effective scattering length $a_\sigma$ close to a Feshbach resonance for a case where the $a_\uparrow = a_\downarrow$ is satisfied within a suitable regime of parameters for Kondo physics given by the boundaries $(c_l, c_u)$ as explained in the text.

 

ultracold atoms with mass $m_a$, $m_b$. Species $a$ is fermionic and is prepared in two different hyperfine states labeled by a spin index $\sigma$. Species $b$, which can be a fermion or boson, is subject to a strong harmonic confining potential. The bound states for the hyperfine states correspond to the unscreened spin in the Kondo problem. In order for the Kondo effect to occur the bound states need to obey certain conditions. First, the bound state between the $a$ and $b$ atoms needs to be well occupied; however, the atoms should not be too tightly bound such that second order spin flip processes—important for the Kondo effect—can occur frequently. This implies a certain regime for the effective scattering lengths $a_\sigma$ bounded by $c_u$ and $c_l$ as shown in Fig. 1(b). Second, the bound state energies should be very similar, since a difference of their energy will favor a certain polarization of the spin, like a magnetic field, which suppresses the Kondo effect. The bound state energies of atoms $a$ with $b$, $E_{b,\sigma}$, generally depend on the scattering lengths $a_\sigma$, $E_{b,\sigma} \simeq -\hbar^2/2m_r a_\sigma^2$, $m_r = m_a m_b/(m_a + m_b)$, and for a general system those will be very different. The challenge is then to find a scheme in which the bound states can be simultaneously tuned to an energy which is roughly equal and in a suitable regime for Kondo physics. As we will show, for certain hyperfine states of a system of $^{40}$K and $^{23}$Na atoms the effective scattering lengths intersect in this regime when tuned close to Feshbach resonances such that Kondo physics is directly possible. However, for many other systems this fortuitous meeting of the conditions will not occur. In the Supplemental Material [23] we show that additional resonances of the confining potential can also be employed to tune the system into the Kondo-correlated state [24,25].

*Physical setup and effective model.*—To formalize these ideas, we first discuss the atomic scattering problem and then relate the parameters to the low energy effective model in Eq. (5), which is directly connected to the Kondo effect. Consider for each component $\sigma$ the two-particle scattering between species $a$ and $b$ described by a Hamiltonian of the form,

$$H_{\text{scat}} = \frac{p_b^2}{2m_b} + \frac{1}{2} m_b \omega_{\text{ho}}^2 r_b^2 + \frac{p_a^2}{2m_a} + V(\boldsymbol{r}_a - \boldsymbol{r}_b), \quad (1)$$

where $\boldsymbol{p}_\alpha$, $\boldsymbol{r}_\alpha$ are momenta and positions of the particles, $V(\boldsymbol{r})$ is the interspecies potential and $\omega_{\text{ho}}$ a scale for the harmonic confinement. A corresponding length scale is the harmonic oscillator length $a_{\text{ho}} = \sqrt{\hbar/m_b\omega_{\text{ho}}}$. The low energy form of the effective $s$-wave scattering amplitude $f_\sigma(k)$ in terms of $a_\sigma$ and the effective radius $r_{e,\sigma}$ is,

$$f_\sigma(k) = \frac{1}{-\frac{1}{a_\sigma} + r_{e,\sigma}\frac{k^2}{2} - ik}. \quad (2)$$

Without the harmonic confinement ($\omega_{\text{ho}} = 0$) the scattering problem for each $\sigma$ is characterized by the bare $s$-wave scattering length $a_{0,\sigma}$. In the presence of the harmonic trap the effective parameters $a_\sigma$ and $r_{e,\sigma}$ can be calculated depending on the bare scattering length $a_{0,\sigma}$ [25,26]. One finds in the Born approximation,

$$a_\sigma = \frac{m_a}{m_r} a_{0,\sigma}, \qquad r_{e,\sigma} = -\frac{m_r}{m_a}\frac{a_{\text{ho}}^2}{a_{0,\sigma}}. \quad (3)$$

To tune the bare scattering lengths $a_{0,\sigma}$ by a magnetic field $B$, we assume that there is a Feshbach resonance,

$$a_{0,\sigma}(B) = a_{\text{bg}}\left(1 - \frac{\Delta B_{0,\sigma}}{B - B_{0,\sigma}}\right), \quad (4)$$

where $a_{\text{bg}}$ is the background scattering length, $\Delta B_{0,\sigma}$ the width and $B_{0,\sigma}$ the position of the resonance.

We describe the low energy physics of the system by an Anderson impurity model (AIM) [27] of the form,

$$H = \sum_{k,\sigma} \varepsilon_k c_{k,\sigma}^\dagger c_{k,\sigma} + \sum_\sigma \varepsilon_{b,\sigma} c_{b,\sigma}^\dagger c_{b,\sigma} + U n_{b,\uparrow} n_{b,\downarrow} + \sum_{k,\sigma} V_{k,\sigma} c_{k,\sigma}^\dagger c_{b,\sigma} + \text{H.c.} \quad (5)$$

Here, $c_{k,\sigma}^\dagger$ creates an itinerant fermion with momentum $\boldsymbol{k}$ and spin projection $\sigma$, and $c_{b,\sigma}^\dagger$ a bound state with energy $\varepsilon_{b,\sigma}$. The states are mixed by the hybridization $V_{k,\sigma}$. Three-particle bound states are assumed to be highly unstable due to rapid decay into deep two-body bound states [28,29]. Under such conditions it has been shown [30] that the system corresponds to $U \to \infty$, where the occupation of those states is suppressed. Particle loss is inhibited in such situations [30]. The effect of the shallow trapping potential on the atoms with mass $m_a$ is neglected, and hence the dispersion is $\varepsilon_k = \hbar^2 k^2/2m_r$ [31]. We focus on the case of three spatial dimensions, where the corresponding density of states (DOS) per spin is $\rho_0(\varepsilon) = c_3\sqrt{\varepsilon}$, with $c_3 = V_0 k_{\text{F}}^3/(4\pi^2\varepsilon_{\text{F}}^{3/2})$, and $\varepsilon_{\text{F}} = (\hbar^2/2m_r)(3\pi^2 n)^{2/3}$. Here, $n = N_a/V_0$, where $V_0$ is the volume of the system and $N_a$ the number of particles of species $a$.

*Relation of AIM parameters to scattering parameters.*—The scattering amplitude is related to the $T$ matrix by

$$f_\sigma(\boldsymbol{k}, \boldsymbol{k}) = -V_0 \frac{m_r}{2\pi\hbar^2} T_{k,k}^\sigma. \quad (6)$$

We can express the right-hand side in terms of scattering properties of the AIM, $T_{k,k}^{\text{A},\sigma}(\omega = \varepsilon_k)$, and from this determine the model parameters in Eq. (5). The $T$ matrix of the AIM is given by [11],

$$T_{k,k'}^{\text{A},\sigma}(\omega) = V_{k,\sigma}^* G_{b,\sigma}(\omega) V_{k',\sigma}, \quad (7)$$

where $G_{b,\sigma}(\omega)$ is the retarded bound state Green's function, $\eta \to 0$,

$$G_{b,\sigma}(\omega)^{-1} = \omega + i\eta - \varepsilon_{b,\sigma} - K_\sigma(\omega) - \Sigma_\sigma(\omega). \quad (8)$$

Generally, impurity properties only depend on the integrated hybridization term $K_\sigma(\omega) = \sum_k (|V_{k,\sigma}|^2/(\omega + i\eta - \xi_k))$, where we defined $\xi_k = \varepsilon_k - \mu$.

A full solution of the scattering problem in Eq. (1) yields $f_\sigma$ [25] such that the AIM parameters can be determined numerically via Eq. (6). Here we take a simplified form, $V_{\boldsymbol{k},\sigma} = V_\sigma$, which is real and constant for $\varepsilon_{\boldsymbol{k}} < \Lambda_{v,\sigma}$ and zero otherwise. This allows us to derive explicit analytical expressions. For generic forms of free states and an $s$-wave bound state, one sees that the overlap integrals $V_{\boldsymbol{k},\sigma}$ vanish when the wavelength $1/k$ becomes much shorter than the typical extension of the bound state $a_\sigma$. From this follows that a reasonable assumption is $\Lambda_{v,\sigma} = (\alpha^2/(k_F a_\sigma)^2)\varepsilon_F$, with $\alpha \simeq 1$, used in the following. From Eq. (6) we find then for small $k$ with Eq. (2) and Eq. (7) with $\mu \to 0$,

$$\frac{V_\sigma^2}{\varepsilon_F^2} = \frac{\frac{8\pi}{V_0 k_F^3}}{\frac{2}{\pi}|k_F a_\sigma| - k_F r_{e,\sigma}}, \tag{9}$$

such that $V_\sigma^2 \sim 1/N_a$ and

$$\frac{\varepsilon_{b,\sigma}}{\varepsilon_F} = \frac{V_0 k_F^3}{4\pi}\left(\frac{2}{\pi|k_F a_\sigma|} - \frac{1}{k_F a_\sigma}\right)\frac{V_\sigma^2}{\varepsilon_F^2} = 2\frac{\frac{2}{\pi|k_F a_\sigma|} - \frac{1}{k_F a_\sigma}}{\frac{2}{\pi}|k_F a_\sigma| - k_F r_{e,\sigma}}. \tag{10}$$

Useful quantities are the hybridization parameter, $\Gamma_\sigma = \pi\rho_0(\varepsilon_F)V_\sigma^2$, which is independent of the volume of the system, and the important ratio

$$\frac{-\varepsilon_{b,\sigma}}{\pi\Gamma_\sigma} = \frac{1}{\pi}\left(\frac{1}{k_F a_\sigma} - \frac{2}{\pi|k_F a_\sigma|}\right), \tag{11}$$

which only depends on $k_F a_\sigma$. We can see how the AIM model parameters depend on $a_\sigma$ and $r_{e,\sigma}$, for instance, $-\varepsilon_{b\sigma}$ increases with $1/a_\sigma$ for $a_\sigma > 0$. As discussed, $a_\sigma$ and $r_{e,\sigma}$ depend on $a_{0,\sigma}$ and thus on the magnetic field $B$ and the trapping frequency $\omega_{ho}$, and this allow us to tune the model parameters in Eq. (5). We see that in general both $h = (\varepsilon_{b,\uparrow} - \varepsilon_{b,\downarrow})/2$, which acts as a local magnetic field, and $\Delta\Gamma = (\Gamma_\uparrow - \Gamma_\downarrow)/2$ can be nonzero. For studies of the AIM the latter is unusual, but it has been discussed in situations of quantum dots coupled to partly polarized leads [32–34]. As discussed in the Supplemental Material, this implies that in general due to second order processes in the hopping an effective local magnetic field $h_{eff}$ is generated. There, also the mapping of the general AIM in Eq. (5) to an anisotropic Kondo model with spin-spin couplings $J_\perp \neq J_z$ and the derivation of the Kondo scale $T_K$ from scaling equations are explained.

*Tuning to the Kondo state.*—We now discuss appropriate parameter regimes to observe the Kondo-correlated state in more detail. These are meant as guidelines and not strict boundaries. The first condition (I) is to have small fluctuations of the occupation of the bound state, which can be expected if $-\varepsilon_{b,\sigma}/(\pi\Gamma_\sigma) > c_1$. A naive estimate is $c_1 \sim 1/2$; however, smaller values, $c_1 \sim 0.25$, also work well as shown later. The second condition (II) is to have the Kondo scale in a regime where it can be observed experimentally, i.e., the experimental temperature $T_{exp} \sim T_K$. We assume $T_{exp} = \alpha_T \varepsilon_F$, where $\alpha_T \sim 0.01$ can be achieved. To achieve this the bound state must not lie too deep. More formally, $T_K$ depends exponentially on the Kondo coupling $J_z$ and the asymmetry $x = J_\perp/J_z < 1$. It follows that $J_z$ must not be too small and the asymmetry should not be too large. These couplings depend on the AIM parameters $\varepsilon_{b,\sigma}$, $\Gamma_\sigma$ (see [23]) and we can obtain a condition of the form $-1/2\sum_\sigma \varepsilon_{b,\sigma}/(\pi\Gamma_\sigma) < c_2$ with a numerical estimate $c_2 \approx 0.6$. Hence, together with (I) we define an interval for values of $-\varepsilon_{b,\sigma}/(\pi\Gamma_\sigma)$, and with the help of Eq. (11) we can state it as a condition for $k_F a_\sigma$,

$$c_l < k_F a_\sigma < c_u, \tag{12}$$

where $c_l = (\pi - 2)/(\pi^2 c_2)$, $c_u = (\pi - 2)/(\pi^2 c_1)$ are lower or upper boundaries [see Fig. 1(b)]. For $\Delta\Gamma \neq 0$, an effective magnetic field is generated, which suppresses Kondo correlations. It is possible to offset the effective field with a local magnetic field $h$, and thus, we define a third condition (III), $\Delta\Gamma = \alpha_h h$. For a symmetric DOS, $\alpha_h \simeq 0.2$ was found numerically [33]; however, for a general DOS and different cutoffs this may vary (see Supplemental Material [23]).

To be able to tune to the Kondo-correlated state, it is necessary to have a system where the Feshbach resonances for $|\uparrow\rangle$ and $|\downarrow\rangle$ with the impurity atom have some overlap. Using the form in Eq. (4) for $a_{0,\sigma}$, $\Delta B_{0,\uparrow}$ and $\Delta B_{0,\downarrow}$ need to have the same sign and $|B_{0,\sigma} + \Delta B_{0,\sigma}| > |B_{0,-\sigma}|$. Given the bare scattering lengths $a_{0,\sigma}$ the effective scattering length including the harmonic potential can be calculated. For simplicity we use the Born approximation in Eq. (3) in the following, which was shown to give reasonably accurate results [25]. Hence, the effective scattering lengths can be tuned close to the Feshbach resonance and it is possible that at the intersection, $a_\uparrow = a_\downarrow$, Eq. (12) is satisfied. This is illustrated in Fig. 1(b). As $a_{0,\uparrow} = a_{0,\downarrow}$, Eq. (3) implies $r_{e,\uparrow} = r_{e,\downarrow}$, such that $h = \Delta\Gamma = 0$ and automatically conditions (I–III) are satisfied. Note that if $a_\uparrow = a_\downarrow$, but $k_F a_\sigma > c_u$, we can satisfy Eq. (12) by reducing the density $n$ and thus $k_F$.

*Experimental system and probe.*—For the experimental realization of our proposal we focus on a system of $^{40}$K with $|\downarrow\rangle \equiv |9/2, -7/2\rangle$ and $|\uparrow\rangle \equiv |9/2, -5/2\rangle$ hyperfine states and $^{23}$Na in the hyperfine state $|1, 1\rangle$. In this system recently molecular states were successfully produced using interspecies Feshbach resonances [20]. For our purpose, the Feshbach resonances with $B_{0,\uparrow} = 106.9$ G, $B_{0,\downarrow} = 108.6$ G, $\Delta B_{0,\uparrow} = -1.8$ G, and $\Delta B_{0,\downarrow} = -6.6$ G [19] are suitable. The background scattering length is $a_{bg} = -690 a_B$, where the Bohr radius is $a_B = 0.53 \times 10^{-10}$ m. In the following we use common values in ultracold gas experiments, $n \sim 10^{18}$ m$^{-3}$, $k_F^0 = [3\pi^2 n]^{1/3} = 1.6 \times 10^{-4}/a_B$. A typical trapping frequency is $\omega_{ho} \sim 100$ kHz [1], such that for $^{23}$Na we have $a_{ho} = 3.12 \times 10^3 a_B$. One has $a_{0,\uparrow} = a_{0,\downarrow} = -1.82 a_{bg}$ for

$$B_s = \frac{B_{0,\downarrow}\Delta B_{0,\uparrow} - B_{0,\uparrow}\Delta B_{0,\downarrow}}{\Delta B_{0,\uparrow} - \Delta B_{0,\downarrow}} = 106.26 \text{ G}. \tag{13}$$

With Eq. (3), this implies $k_F^0 a_\sigma = 0.55$. Employing the numerical renormalization group (NRG) [35,36], we calculated the low temperature bound state spectral function, $\rho_{b,\sigma}(\omega)$, for parameters corresponding to the K-Na system for the situation where $B = B_s$ in Eq. (13) and we vary $k_F/k_F^0$, where $k_F^0$ is as above. The energy scale is set by $\varepsilon_F = 1$, and we measure all energies from $\varepsilon_F$. The numerical values for the AIM parameters are given in Table I in the Supplemental Material. The result is shown in Fig. 2(a). The bound state peaks lie between $-8\varepsilon_F$ (not shown) and $-2\varepsilon_F$. Because of interaction effects the peaks are broadened, even though they lie outside the continuum; however, the width might be overestimated in the NRG calculation. At $\omega = 0$ we see a clear peak, the Kondo or Abrikosov-Suhl resonance. We can extract the half width of the Kondo resonance $\Delta_K \sim 0.1\varepsilon_F$, which is indicative of the Kondo scale suitable for experimental observations.

We will now describe experimental signatures to detect the Kondo-correlated state. The retarded Green's function of itinerant states in the presence of $n_{\mathrm{imp}}$ impurities is given by [11],

$$G_{\boldsymbol{k},\sigma}(\omega)^{-1} = \omega + i\eta - \xi_{\boldsymbol{k}} - n_{\mathrm{imp}} V_\sigma^2 G_{b,\sigma}(\omega), \qquad (14)$$

and $\rho_{\boldsymbol{k},\sigma}(\omega) = -(1/\pi)\,\mathrm{Im}G_{\boldsymbol{k},\sigma}(\omega)$, $\eta \to 0$, is the momentum resolved spectral function. In ultracold gas experiments, $\rho_{\boldsymbol{k},\sigma}(\omega)$ can be measured directly by momentum resolved photoemission spectroscopy [37–39]. For an impurity concentration $n_{\mathrm{imp}}/N_a \approx 0.03$ and parameters corresponding to $\varepsilon_b/\pi\Gamma = -0.21$ in Fig. 2(a), we show $\rho_{\boldsymbol{k},\sigma}(\omega)$ in Fig. 2(b). The change of the height and width of the peaks when approaching $k_F$ can be easily understood as due to the coupling of the itinerant states to the Kondo resonance. In Eq. (14) the imaginary part of $G_{b,\sigma}(\omega)$, which is proportional to the spectral function $\rho_{b,\sigma}(\omega)$ leads to a broadening of the spectral function, which is most pronounced close to $\varepsilon_{\boldsymbol{k}} = \varepsilon_F$, where the Kondo resonance lies. This is a striking feature opposite to the usual

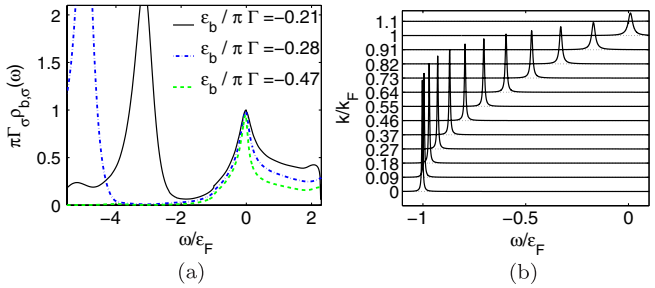


FIG. 2 (color online). (a) Spectral function $\rho_{b,\sigma}(\omega)$ for different values of $\varepsilon_{b,\sigma}/\pi\Gamma$ obtained for $k_F = 1$, 0.75, $0.45k_F^0$. The corresponding values are $k_F a_\sigma = 0.55$, 0.41, 0.25 and the complete set of AIM parameters is given in Table I in the Supplemental Material. The magnetic field $B$ has been tuned such that $a_\uparrow = a_\downarrow$. (b) Momentum resolved spectral function $\rho_{\boldsymbol{k},\sigma}(\omega)$ as calculated from Eq. (14) for the case $\varepsilon_b/\pi\Gamma = -0.21$ with $n_{\mathrm{imp}}$ as discussed below Eq. (14).

scattering mechanisms which increase when moving away from the Fermi energy. In fact, we can interpret this is as a self-energy term, $\Sigma(\omega) = n_{\mathrm{imp}} V_\sigma^2 G_{b,\sigma}(\omega)$, and this can be extracted [40] by well established techniques developed in angle-resolved photo emission spectroscopy [41,42]. Hence, this procedure gives access to the spectral function in Fig. 2(a) and as such is a direct signature of the Kondo peak. More conventional radio frequency (rf) spectroscopy can also provide explicit signatures of the Kondo-correlated state. As discussed comprehensively in the Supplemental Material [23], the signal shows characteristic broadened peaks, which are shifted from the ones for a system without the Kondo effect. Also spectroscopy of the species $b$ impurity atom, switching from an uncorrelated state to a Kondo state, would be very interesting. Characteristic power law tails can be observed as discussed in detail in Refs. [43,44].

*Addressing open questions.*—We discuss now a number of interesting questions, which can be addressed once the Kondo-correlated state has been realized. It has been long argued [11] that the magnetically screened impurity should be surrounded by a screening cloud with the spatial extension of order $\xi_K = (\hbar v_F/k_B T_K)$. However, experimentally it has not been possible to provide firm evidence for the Kondo cloud, such that its existence is unclear. A typical quantity to show Kondo cloud features is the decay of the equal time spin correlation function $\langle S_c(\boldsymbol{r}) s_{\mathrm{imp}}\rangle$, which is difficult to access in condensed matter systems. In contrast, in the proposed ultracold gas system this correlation function should become accessible by spectroscopic tools [45], such that $\xi_K$ could be determined and this fundamental question of Kondo physics be settled. Since our setup allows us to switch the impurity on and off by optically changing the hyperfine state of the $b$ species, it would also be curious to analyze the time scale on which the Kondo cloud builds up. The proposed setup has also great potential to shed light on a number of intriguing issues for the Kondo lattice including the observation of a fractionalized Fermi liquid (FL*) phase [46] and the occurrence of superconductivity close to a quantum phase transitions.

*Conclusions.*—We have demonstrated how to realize a Kondo-correlated state for a mixture of ultracold atoms. The proposed setup, different from a previous proposal based on alkaline-earth atoms [47], ones related to the spin-Boson model [48,49] and a bosonic form [50], can be realized with experimental techniques currently available. In general, this allows one to analyze field dependent and anisotropic Kondo physics. We proposed the recently studied Na-K-mixture as a suitable system and computed the rf response in a regime well accessible by experiments. There are numerous possible extension of our work including the study of nonequilibrium Kondo physics, Kondo lattice systems and signatures of quantum criticality. We point out that geometrical resonances which we discuss in the Supplemental Material [23] can also appear in $l > 0$ angular momentum channels even for purely $s$-wave

scattering between localized and itinerant atoms (see, e.g., [25,26]). This may open interesting possibilities for realizing multichannel Kondo physics.

We wish to thank S. Blatt, S. Gopalakrishnan, A. C. Hewson, M. Koehl, Y. Oreg, M. Punk, S. Will, A. Tsvelik, G. Zarand, F. Zhou, and M. Zwierlein for helpful discussions. We would like to thank Martin Zwierlein for pointing out to us the possibility of using Feshbach bound states on impurity atoms to realize the Kondo effect in cold atomic systems and for a collaboration on related projects [51]. J. B. acknowledges financial support from the DFG through Grant No. BA 4371/1-1. We also acknowledge support from Harvard-MIT CUA, DARPA OLE program, AFOSR Quantum Simulation MURI, AFOSR MURI on Ultracold Molecules, the ARO-MURI on Atomtronics, ARO MURI Quism program and the EU ERC Ferlodim.

[1] I. Bloch, J. Dalibard, and W. Zwerger, Rev. Mod. Phys. **80**, 885 (2008).
[2] W. Hofstetter, J. I. Cirac, P. Zoller, E. Demler, and M. D. Lukin, Phys. Rev. Lett. **89**, 220407 (2002).
[3] M. Greiner, O. Mandel, T. Esslinger, T. W. Hansch, and I. Bloch, Nature (London) **415**, 39 (2002).
[4] M. Greiner, C. Regal, and D. Jin, Nature (London) **426**, 537 (2003).
[5] M. Zwierlein, J. Abo-Shaeer, A. Shirotzek, C. H. Schunck, and W. Ketterle, Nature (London) **435**, 1047 (2005).
[6] J. K. Chin, D. E. Miller, Y. Liu, C. Stan, W. Setiawan, C. Sanner, K. Xu, and W. Ketterle, Nature (London) **443**, 961 (2006).
[7] U. Schneider, L. Hackermuller, S. Will, T. Best, I. Bloch, T. A. Costi, R. W. Helmes, D. Rasch, and A. Rosch, Science **322**, 1520 (2008).
[8] R. Jordens, N. Strohmaier, K. Gunter, H. Moritz, and T. Esslinger, Nature (London) **455**, 204 (2008).
[9] D. Goldhaber-Gordon, H. Shtrikman, D. Mahalu, D. Abusch-Magder, U. Meirav, and M. A. Kastner, Nature (London) **391**, 156 (1998).
[10] S. M. Cronenwett, T. H. Oosterkamp, and L. P. Kouwenhoven, Science **281**, 540 (1998).
[11] A. C. Hewson, *The Kondo Problem to Heavy Fermions* (Cambridge University Press, Cambridge, England, 1993).
[12] I. Affleck and P. Simon, Phys. Rev. Lett. **86**, 2854 (2001).
[13] L. Borda, Phys. Rev. B **75**, 041307 (2007).
[14] I. Affleck, L. Borda, and H. Saleur, Phys. Rev. B **77**, 180404 (2008).
[15] Q. Si and F. Steglich, Science **329**, 1161 (2010).
[16] H. v. Löhneysen, A. Rosch, M. Vojta, and P. Wölfle, Rev. Mod. Phys. **79**, 1015 (2007).
[17] T. Köhler, K. Góral, and P. S. Julienne, Rev. Mod. Phys. **78**, 1311 (2006).
[18] C. Chin, R. Grimm, P. Julienne, and E. Tiesinga, Rev. Mod. Phys. **82**, 1225 (2010).
[19] J. W. Park, C.-H. Wu, I. Santiago, T. G. Tiecke, S. Will, P. Ahmadi, and M. W. Zwierlein, Phys. Rev. A **85**, 051602 (2012).
[20] C.-H. Wu, J. W. Park, P. Ahmadi, S. Will, and M. W. Zwierlein, Phys. Rev. Lett. **109**, 085301 (2012).
[21] S.-K. Tung, C. Parker, J. Johansen, C. Chin, Y. Wang, and P. S. Julienne, Phys. Rev. A **87**, 010702 (2013).
[22] M. Repp, R. Pires, J. Ulmanis, R. Heck, E. D. Kuhnle, M. Weidemüller, and E. Tiemann, Phys. Rev. A **87**, 010701 (2013).
[23] See Supplemental Material at http://link.aps.org/supplemental/10.1103/PhysRevLett.111.215304 for additional details which complement the main text.
[24] M. Olshanii, Phys. Rev. Lett. **81**, 938 (1998).
[25] P. Massignan and Y. Castin, Phys. Rev. A **74**, 013616 (2006).
[26] Y. Nishida and S. Tan, Phys. Rev. A **82**, 062713 (2010).
[27] P. W. Anderson, Phys. Rev. **124**, 41 (1961).
[28] E. Braaten and H.-W. Hammer, Phys. Rep. **428**, 259 (2006).
[29] T. Kraemer *et al.*, Nature (London) **440**, 315 (2006).
[30] N. Syassen, D. Bauer, M. Lettner, T. Volz, D. Dietze, J. Garcia-Ripoll, J. Cirac, G. Rempe, and S. Dürr, Science **320**, 1329 (2008).
[31] This is justified by the local density approximation, which is usually a good description for trapped systems.
[32] J. Martinek, Y. Utsumi, H. Imamura, J. Barnaś, S. Maekawa, J. König, and G. Schön, Phys. Rev. Lett. **91**, 127203 (2003).
[33] J. Martinek, M. Sindel, L. Borda, J. Barnaś, J. König, G. Schön, and J. von Delft, Phys. Rev. Lett. **91**, 247202 (2003).
[34] M.-S. Choi, D. Sánchez, and R. López, Phys. Rev. Lett. **92**, 056601 (2004).
[35] K. Wilson, Rev. Mod. Phys. **47**, 773 (1975).
[36] R. Bulla, T. Costi, and T. Pruschke, Rev. Mod. Phys. **80**, 395 (2008).
[37] T.-L. Dao, A. Georges, J. Dalibard, C. Salomon, and I. Carusotto, Phys. Rev. Lett. **98**, 240402 (2007).
[38] J. Stewart, J. Gaebler, and D. Jin, Nature (London) **454**, 744 (2008).
[39] M. Feld, B. Fröhlich, E. Vogt, M. Koschorreck, and M. Köhl, Nature (London) **480**, 75 (2011).
[40] The energy resolution required is set by the peak width in Fig. 2(b). For $n_{\mathrm{imp}}/N_a \sim 0.1$ the width at $k = k_{\mathrm{F}}$ is $\Delta/\varepsilon_{\mathrm{F}} \sim 0.09$.
[41] T. Valla, A. V. Fedorov, P. D. Johnson, B. O. Wells, S. L. Hulbert, Q. Li, G. D. Gu, and N. Koshizuka, Science **285**, 2110 (1999).
[42] A. Damascelli, Z. Hussain, and Z.-X. Shen, Rev. Mod. Phys. **75**, 473 (2003).
[43] C. Latta *et al.*, Nature (London) **474**, 627 (2011).
[44] M. Knap, A. Shashi, Y. Nishida, A. Imambekov, D. A. Abanin, and E. Demler, Phys. Rev. X **2**, 041020 (2012).
[45] M. Knap, A. Kantian, T. Giamarchi, I. Bloch, M. D. Lukin, and E. Demler, Phys. Rev. Lett. **111**, 147205 (2013).
[46] T. Senthil, S. Sachdev, and M. Vojta, Phys. Rev. Lett. **90**, 216403 (2003).
[47] A. Gorshkov, M. Hermele, V. Gurarie, C. Xu, P. Julienne, J. Ye, P. Zoller, E. Demler, M. Lukin, and A. Rey, Nat. Phys. **6**, 289 (2010).
[48] A. Recati, P. O. Fedichev, W. Zwerger, J. von Delft, and P. Zoller, Phys. Rev. Lett. **94**, 040404 (2005).
[49] P. P. Orth, I. Stanic, and K. Le Hur, Phys. Rev. A **77**, 051601 (2008).
[50] G. M. Falco, R. A. Duine, and H. T. C. Stoof, Phys. Rev. Lett. **92**, 140402 (2004).
[51] E. Vernier, D. Pekker, M. W. Zwierlein, and E. Demler, Phys. Rev. A **83**, 033619 (2011).